

Histopathological Impact of Ginger Loaded Nanoparticle Versus Ginger Extract as A Novel Therapy of Experimentally Induced Acute Ulcerative Colitis

Original
Article

Manal H. Al-Badawi¹, Nermien E. Waly², May M. Eid³ and Nahed A. Soliman⁴

¹Department of Human Anatomy and Embryology, ²Department of Physiology, ⁴Department of Pathology, Faculty of Medicine, Helwan University, Helwan, Egypt.

³Spectroscopy Department (Physics Division), National Research Centre, Dokki, Egypt.

ABSTRACT

Background: Ulcerative colitis (UC) is a debilitating chronic inflammatory bowel disease that is prevalent in Egypt. Current treatment of UC is expensive and has serious side effects.

Aim of the Work: To evaluate the effect of ginger loaded nanoparticles (GDNP) compared to ginger extract (GE) as an alternative treatment of acute UC (AUC) in DSS/ ethanol rat model.

Material and Methods: Twenty rats were used. AUC was induced by administration of 2% synthetic dextran sulfate sodium (DSS). Rats were divided into 4 groups: control (GP I), AUC (GP II), AUC received 2.5 gm GE (GP III) and AUC received 2.5 gm superparamagnetic@ silver nanoparticles GDNP (GP VI). Colonic and rectal tissue were assessed histologically using Hematoxylin and eosin (H&E), Periodic acid- Schiff (PAS), Toluidine blue, and electron microscopy (EM). Epithelial proliferation and apoptosis were assessed by anti-KI-67 antibody anti BCL2 antibody.

Results: GP III and GP IV showed improvement with GDNP and GE compared to control. Gross damage scores were as follows: GP I 0±0, GP II 2.6±1.1, GP III 1.4±1.1, and GP IV 0±0 with significant variation (P = 0.000). Cumulative histopathological score of GP I, II, III, and IV were 0±0, 9.2±3.3, 3±1.6, and 1±1 respectively with significant correlation (P= 0.000). GP III and GP IV displayed strong positive nuclear and cytoplasmic staining for KI-67 (GP III Mean=50±15/ HPF). (GP IV Mean=66±8/ HPF) and BCL2 (Mean=60±16 and 76±9/ HPF) with significant variation (P= 0.000).

Conclusion: GDNP has more potential in treatment of AUC compared to GE. Treatment with GDNPs improved signs, reduced apoptosis and enhanced repair of AUC more significantly

Received: 19 March 2021, **Accepted:** 17 April 2021

Key Words: BCL2, ginger, ginger loaded nanoparticles, KI-67, ulcerative colitis.

Corresponding Author: Manal H. Al Badawi, MD, Department of Human Anatomy and Embryology, Faculty of Medicine, Helwan University, Helwan, Egypt, **Tel.:** +20 11436 11663, **E-mail:** manalalbadawi@yahoo.com

ISSN: 1110-0559, Vol. 45, No.2

INTRODUCTION

Ulcerative colitis (UC) is a debilitating chronic inflammatory bowel disease (IBD) that is more common in young women^[1-3]. Although more prevalent in western countries, a sharp rise of the UC incidence has been observed in developing countries including Egypt over the last decade^[4]. UC is characterized by remission and relapse of diarrhea, abdominal pain and bloody stool. It often starts at the rectum and extends proximally to involve the entire colon^[5-7]. Although not very clear, several factors have been described to play a role in the pathophysiology of UC e.g., intestinal microbiota, epithelial function, mucosal immunity and genetic susceptibility^[2,6-8]. It is thought that these factors result in increased production of reactive oxygen species (ROS) and decreased antioxidant activity with the consequent colonic inflammation^[7,9].

Pathologically, acute UC is characterized by red, granular-mucosa and huge broad-based ulcers. Ulcers are aligned along the long axis of the colon. Pseudo-polyps

are isolated islands of regenerating mucosa that bulge into the lumen. Chronic disease may lead to mucosal atrophy. The hallmark in UC is inflammation that is limited to the mucosa and submucosa together with dense infiltration of neutrophils and macrophages together with crypt abscess and distortion^[2,5,10]

Current conventional medical treatment of UC includes both anti-inflammatory and immunosuppressant drugs. These drugs have many life-threatening side effects such as infection and increased risk malignancy^[6,7,11]. Lately, targeted therapy has been developed, against inflammatory responses in UC particularly anti TNF- α and selective adhesion molecules inhibitors. However, the use of such therapies is limited by serious side effects and high cost as well as systemic administration^[11,12].

As current pharmacological treatment poses many limitations research is geared toward finding alternative therapeutics. Herbs has been used in traditional and folk medicine as a treatment for many diseases including control

and prevention of UC^[7-9,13]. Ginger, *Zingiber Officinale* Rosc., is one of the widely used dietary supplements in traditional medicine^[14]. Ginger rhizomes contains a zerurnbone that has anticancer and antioxidant actions^[15,16]. Ginger extract has anti-inflammatory effects and protects against ulcer development in albino rats^[17,18]. Ginger active component (gingerols, shogaols) has antioxidative, anti-inflammatory, and anticarcinogenic properties and it effectively reduced colitis^[11,19]. It is safe to use with its LD50 of about to 1 g/kg^[20].

Nano particles-based drug-delivery systems were recently developed and, in a trial, to improve therapeutic outcome of UC. This approach saves the loaded drug from environmental degradation, increases its solubility, augments its^[21] absorption, reducing systemic toxicity and enables sustained release of the drug and thus massively improve UC treatment^[13,19,22,23].

The objective of this study is to evaluate of the effect and potential use of ginger derived nanoparticles (GDNP) compared to ginger extract (GE) as a treatment of acute UC in DSS/ ethanol rat model^[24].

MATERIAL AND METHODS

Animals

Twenty- specific pathogen-free adult male albino rats (180-250 gm) average age 8 weeks. Animal Breeding Core Helwan, were maintained (two or three per cage) in isolator plastic cages with shavings under standard laboratory conditions (sterilizable diet, 50% humidity, 23-24°C temperature, and 12 hours light/12 hours dark cycle). All rats were quarantined 2 weeks after arrival and then randomized by body weight into experimental and control groups. All the rats were permitted free access to a commercial diet and normal drinking tap water in individual bottles. All procedures conformed to the guidelines established by the animal house of Ain Shams University and were approved by the Ethical Committee of Helwan University. No set criteria were used to exclude or include animals from the study. Only Authors were aware of groups allocations and treatment.

Materials

Iron (II) chloride-hexahydrate (FeCl₃ · 6H₂O), Ammonium iron (II) sulfate hexahydrate (NH₄)₂Fe(SO₄)₂ · 6H₂O were purchased from Merck (Germany) and used as received without any purifications.

Preparation of NPs (Production of fungal biomass and Intracellular synthesis of superparamagnetic iron oxide@ Silver nanocomposites (SPION@Ag).

SPION@Ag were prepared through a green route, we employed a fungal species, *Fuzarium oxyporium* that were isolated from soil samples that have been previously collected from local areas in Egypt. For the production of fungal biomass, flasks containing potato dextrose broth were inoculated with fungal isolates at 25°C, under shaking condition (180 rpm). The fungal filtrates were carefully separated from the mycelia, under antiseptic conditions. The seeds of AgNPs were prepared as follow: 2 mM AgNO₃ were added to 50 ml fungus filtrates, with vigorous shaking at 37 °C. The solution of FeO NPs seeds were prepared as following: 5mM FeCl₃ and 2.5 mM Fe(SO₄)₂ were mixed in 50 ml sterile distilled water and the pH adjusted to 12.5 under vigorous shaking at at 80°C, C:10mM FeCl₃ and 5 mM Fe(SO₄)₂ were mixed in 50 ml sterile distilled water and the pH adjusted to 12.5 under vigorous shaking at 80 °C. The two solutions were mixed under shaking at 37 °C for 72 hours. The nanoparticles were washed and the formations of the core shell were examined by UV/Visible and FTIR spectroscopy^[25-28].

Preparation and Characterization of Ginger derived nanoparticles (GDNP)

50 gm of fresh ginger were washed, dried and blended. The blended extract was set up to 200 ml using distilled water the centrifuged @3000 gm for 29 min then the supernatant was centrifuged to 10000gm for 40 min. The supernatant was separated and sonicated with 1 mg/ml SPION@Ag for 10 sec.

Molecular vibration of ginger and NPs functionalized with ginger were assigned in (Figure 1a). The ginger functional groups were assigned for amide I and amide II at 1640, and 1540 cm⁻¹, the Aromatic skeletal combined with C–H in-plane deforming and stretching was assigned at 1414cm⁻¹, the CH₃ asymmetric stretching at 1138 cm⁻¹^[29]. The NPs functionalized with ginger spectrum show the disappearance of amide II NH₂ band, and the appearance of new band at 1020 cm⁻¹, and the appearance of the Fe-O band at 540 cm⁻¹. The significant change in the ginger spectrum is attributed to the formation of bonds between NPs and the functional groups of ginger. The UV/Visible spectrum of ginger and NPs functionalized with ginger were reported at (Figure 1b) confirming the immobilization of ginger on the surface of NPs. (Figure 1c) shows the high-resolution transmission electron microscope (HRTEM) of superparamagnetic NPs (SPION)@Ag core shell (a), and the SPION@Ag functionalized with ginger(b). (Figure 1d) confirms the spherical shape of ginger-functionalized SPION with particle size less then 50 nm.

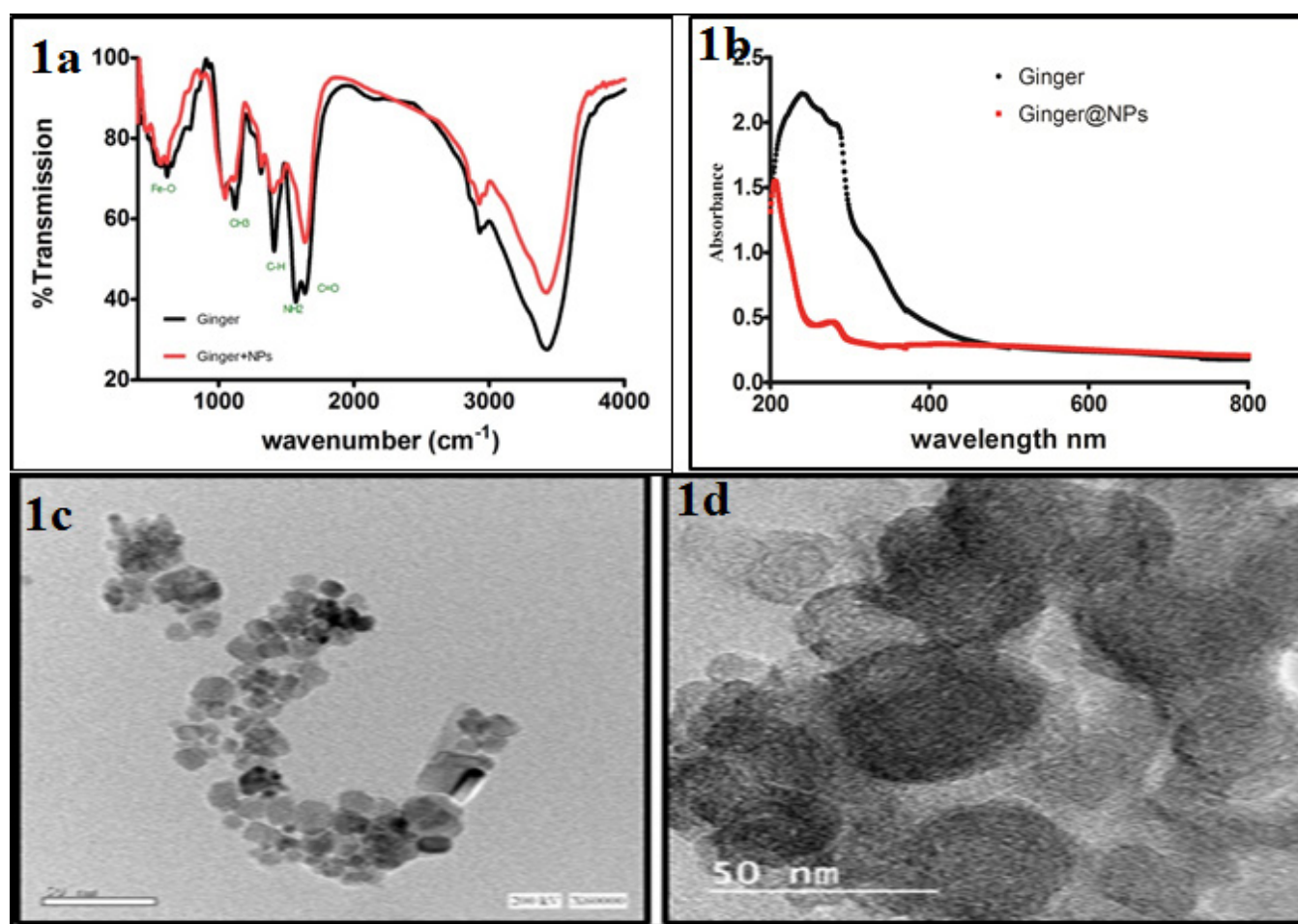


Fig. 1: a: FTIR spectrum of Ginger and NPs functionalized with Ginger. The spectrum shows the disappearance of amide II band (NH₂) from the ginger spectrum and the formation of a new band at 1020 cm⁻¹ and confirm the FeO band at 540 cm⁻¹. b: UV/Visible spectrum of Ginger and NPs functionalized with Ginger. There is disappearance of the C-C band of ginger at 280 nm and the appearance of a shoulder at 300 nm at the spectrum of Ginger @NP. c,d: HR-TEM of NPs, and NPs functionalized with NPs. The NPs on the left show the spherical SPION@Ag with size < 50 nm on the right the SPION were functionalized with ginger.

Induction of acute ulcerative colitis and its evaluation

Experimental acute colitis was induced to rats by repeated administrations of 2% (wt/ vol; 20 g/L) 2 % synthetic dextran sulfate sodium (DSS) (MW 5000 Da, Sigma, USA) in drinking tap water for 3 days. A rubber catheter (OD, 2 mm) was inserted rectally into the colon such that the tip was 8 cm proximal to the anus, approximately at the splenic flexure. Intra-rectal administration of 0.5 ml Ethanol (50% dilution) via the catheter. This dose was empirically reported to induce moderate to severe colitis with minimal mortality in rats. The changes in growth rate, stool consistency and presence of gross bleeding were assessed during the experiment to evaluate the disease activity^[6,24].

Study Design

Acute ulcerative colitis was induced in rats as described above. Experimental groups were divided as follows:

- **Group I (Control group):** rats received standard rat diet and received distilled water during the whole experiment.

- **Group II (acute UC):** UC induced rats in this group received no treatment.
- **Group III (Treated acute UC by ginger extract):** UC induced rats in this group received 2.5 mg of ginger extract alone.
- **Group IV (Treated acute UC by GDNP):** UC induced rats in this group received 2.5 mg of ginger loaded nanoparticles.

Tissue preparation

The animals were sacrificed by cervical dislocation two hours after the last administration (optimal time for the inflammatory reaction in the colon demonstrated by histological analyses. Distal colon and rectum were excised and examined grossly for hyperemia, erosion/ulceration, and the presence of thickening of the wall. The sum of the scores of the three parameters represented the mucosal damage score in each animal according to Chen *et al.*, 2007^[24]. Then the dissected colon was washed with cooled PBS and fixed in 10% PBS- buffered formalin for 24 h. After paraffin embedding, 4- μ m thick transverse sections of the tissues were obtained, stained with

hematoxylin and eosin (H&E) and Periodic acid - Schiff (PAS) then examined under a light microscope. One fresh tissue sample was fixed in glutaraldehyde for electron microscopic examination.

Histopathology and Immunohistochemistry

The sections were stained with H&E and examined with light microscope. Sections were assessed for parameters of active colitis. These parameters include destruction of epithelium and glands, dilation of glandular crypts, Depletion and loss of goblet cells, inflammatory cells infiltration, edema, Hemorrhagic mucosa, and Crypt abscesses. Each parameter was given a score from 0 to 3 based on the distribution of the lesion as focal, zonal, and diffuse. Cumulative histopathological score (6 sections per rat) of individual rats represents the sum of the sub-scores of the different histological parameters^[24].

IHC examination was performed using a Ventana Benchmark Ultra machine automated staining system. The primary antibodies used were cell marque Ki-67 (sp6) rabbit monoclonal antibody (REF275R-18), anti BCL2 mouse monoclonal primary antibody (DAKO Clone 124). KI67 staining pattern is nuclear whoever BCL2 staining pattern is nuclear and cytoplasmic. We calculated the ratio of anti-Ki-67 and anti-BCL2 positive cells to the total cell count in the crypt in an attempt to evaluate the apoptosis and cell cycle status in the model of acute ulcerative colitis and after administration of different therapeutic approaches (ginger alone, and ginger NPs)^[24]. Adjacent normal colonic epithelium and lymphocytes served as positive internal controls. Negative controls were done via replacing primary antibody with PBS.

Electron microscopy

Tissue specimens of the colon were divided into small pieces of 1 mm³ in size, fixed in 2.5% glutaraldehyde, dehydrated and transferred on the next day into the tip of an individually labeled capsule. Semithin sections of 0.5-1 mm thickness were obtained, stained with toluidine blue and examined with light microscopy, and ultra-thin sections of 60 nm to 100 nm in thickness were obtained, contrasted with uranyl acetate and lead citrate and examined with electron microscopy (Transmission Electron Microscope at the Regional Center for Mycology and Biotechnology Transmission Electron Unit, 1 Azhar University, Cairo, Egypt) and photographed using a Jeol-1010 (Jeol, Tokyo, Japan).

Morphometric study

We used Leica Qwin 500" software image analyzer computer system (Leica image system Ltd; Cambridge, England), with an objective lens of x40 magnification, whereas 10 non-overlapping randomly chosen fields were studied for each section. The following parameters were measured:

- a. The number of PAS positive goblet cells.
- b. The number of mast cells stained with Toluidine blue.

- c. The quantity anti-Ki-67 and anti BCL2 positive cells, the ratio of anti-Ki-67 anti BCL2 positive cells to the total cell count in the crypt.

Statistical analysis

All statistical analyses were done using the SPSS version20 software program. The data tested by Kolmogorov-Smirnov Z. test to detect them parametric or non. All data were parametric and continuous. No data points were excluded. All data were described using means \pm standard deviation. ONE WAY ANOVA TEST was performed to compare the means of all variables among the studied groups. Differences were regarded as statistically significant at $P < 0.05$.

RESULTS

Clinical evaluation

Gross bleeding and loose stool/diarrhea were observed in all rats received DSS (GP II, III, IV before treatment). These are the main signs of UC and represented the main sign of success of the model, while the rats in GP I didn't show any of these signs.

Gross appearance examination

Gross appearance of the resected colon of GP II revealed erosive and hemorrhagic mucosa at single or multiple sites but never proximal to the splenic flexure. No gross thickening of the colonic wall which is an indication of limited inflammation macroscopically. The gross observation of the resected colon of GPI revealed intact mucosa. The gross observation of the resected colon of GP III and IV revealed slight hyperemia without erosion, ulceration, or any sign of inflammation. The gross damage scores of GP I, II, III, and IV were 0 ± 0 , 2.6 ± 1.1 , 1.4 ± 1.1 , 0 ± 0 respectively with significant variation ($P = 0.000$) (Figure 2, Table).

Histopathological studies

H&E

Sections prepared from the colon of the control group (GP I) showed normal mucosa, submucosa, muscosa and serosa. The mucosa was folded and lined by simple columnar epithelial cells with goblet cells. The sections prepared from the colon of the acute UC group (GPII) displayed erosion of the mucosa, near absence of goblet cells, and malformed widely spaced crypts. Mixed inflammatory cells infiltration in the mucosa and in the submucosa was present particularly neutrophils and eosinophils. Sections prepared from the colon of the ginger treated acute UC group (GP III) showed mostly normal folded mucosa lined by surface columnar epithelial cells with a moderate number of goblet cells and near closely regular crypts. Fewer inflammatory cells infiltrate was present in the crypt base and lamina propria and not extending beyond the muscularis mucosa. Sections prepared from the colon of the ginger loaded with nanoparticle treated acute UC group (GP IV) showed a normal folded mucosa lined by surface columnar epithelial

cells with a huge number of goblet cells and closely regular crypts. Very limited to absent inflammatory cells infiltrate in the mucosa and submucosa (Figure 3).

The mean number of goblet cells in the studied groups was as follows: GP I 19/HPF, GP II 0.4/HPF, GP III 33/HPF, and GP IV 73/HPF (Figure 9).

Cumulative histopathological score of GPI, II, III, and IV were 0 ± 0 , 9.2 ± 3.3 , 3 ± 1.6 , and 1 ± 1 respectively with a significant correlation ($P = 0.000$) (Table).

PAS

Section from the GP I exhibited numerous PAS-positive goblet cells in the crypts of colonic mucosa (Mean = 19/HPF). GP II did not reveal PAS-positive goblet cells (Mean = 0.4/HPF). GP III displayed many PAS-positive goblet cells (Mean = 33/HPF). GPIV showed a huge number of goblet cells (Mean = 73/HPF) (Figures 4C, 9). There was significant variation in the number of goblet cells among the studied groups ($P = 0.000$) (Table and Figures 4,9).

Toluidine blue

Mast cells were not present in the mucosa and submucosa of the colons from the control rats. GP II showed numerous mast cells with toluidine blue positive reaction in the lamina propria and submucosa. In GP III, and G IV, there were very few mast cells in the colonic mucosa. The mean number of mast cells in GPI, GP II, GP III and GPIV were 0.4, 21, 11, 7/HPF respectively (Figures 5,9). There was a statistically significant variation of the number of mast cells among the studied groups ($P = 0.000$) (Table).

Electron microscopic analysis

Electron microscopic figures of the resected colon from GP I revealed a closely regular crypt lined by simple columnar epithelial cells with excess number of goblet cells. GP II revealed malformed widely spaced crypts with absent goblet cells and heavy neutrophilic (segmented) nuclei and an eosinophilic (bilobed) nuclei infiltration around and invading the crypt epithelial cells. GP III revealed closely regular crypts lined by columnar epithelial cells with an excess number of goblet cells and a little inflammatory cell infiltration compared to the AUC model. GP IV revealed closely packed crypts lined by columnar epithelial cells with a huge number of goblet cells (cup shaped appearance) without an inflammatory cell infiltration. (Figure 6).

Immunohistochemistry

GP I revealed a positive moderate nuclear staining for KI-67 (Mean = 20 ± 7 /HPF) (Figure 7A). GP II showed near absent week positive nuclear staining for KI67

(Mean = 5 ± 3.6 /HPF) mostly sparing the crypt (Figure 7B, Table). GP III (AUC treatment by ginger) displayed a strong positive moderate nuclear staining for KI67 (Mean = 50 ± 15 /HPF) (Figure 7C, Table). GP IV revealed a strong positive moderate nuclear staining for KI67 (Mean = 66 ± 8 /HPF) (Figure 7D, Table). A statistically significant variation of the mean of KI67 positive cells ratio was noticed among the different groups in the study ($P = 0.000$) (Table).

GP I revealed a positive moderate nuclear and cytoplasmic staining for BCL2 (Mean = 25 ± 8 /HPF). GP II showed a weak positive nuclear and cytoplasmic staining for BCL2 (Mean = 8 ± 4.6 /HPF) mostly sparing the crypt. GP III displayed strong positive moderate nuclear and cytoplasmic staining for BCL2 (Mean = 60 ± 16 /HPF). GP IV revealed strong positive moderate nuclear and cytoplasmic staining for BCL2 (Mean = 76 ± 9 /HPF). There was a significant variation of the mean of BCL2 positive cells ratio among the different groups in the study (One Way ANOVA $P = 0.000$) (Figures 8,10 and Table).



Fig. 2: Photographs of sections in the rat colons of the different groups. from the different studied groups; GP I(Control) showing an intact mucosa, no hyperaemia or erosion/ulceration. GP II (AUC) showing severe hyperaemia with mild thickening of the mucosa(yellow *). Treated groups with ginger extract (GE) and ginger derived nanoparticles (GDNP) GPIII (GE), and GPIV (GDNP) showing intact mucosa, no erosion/ ulceration or thickened wall.

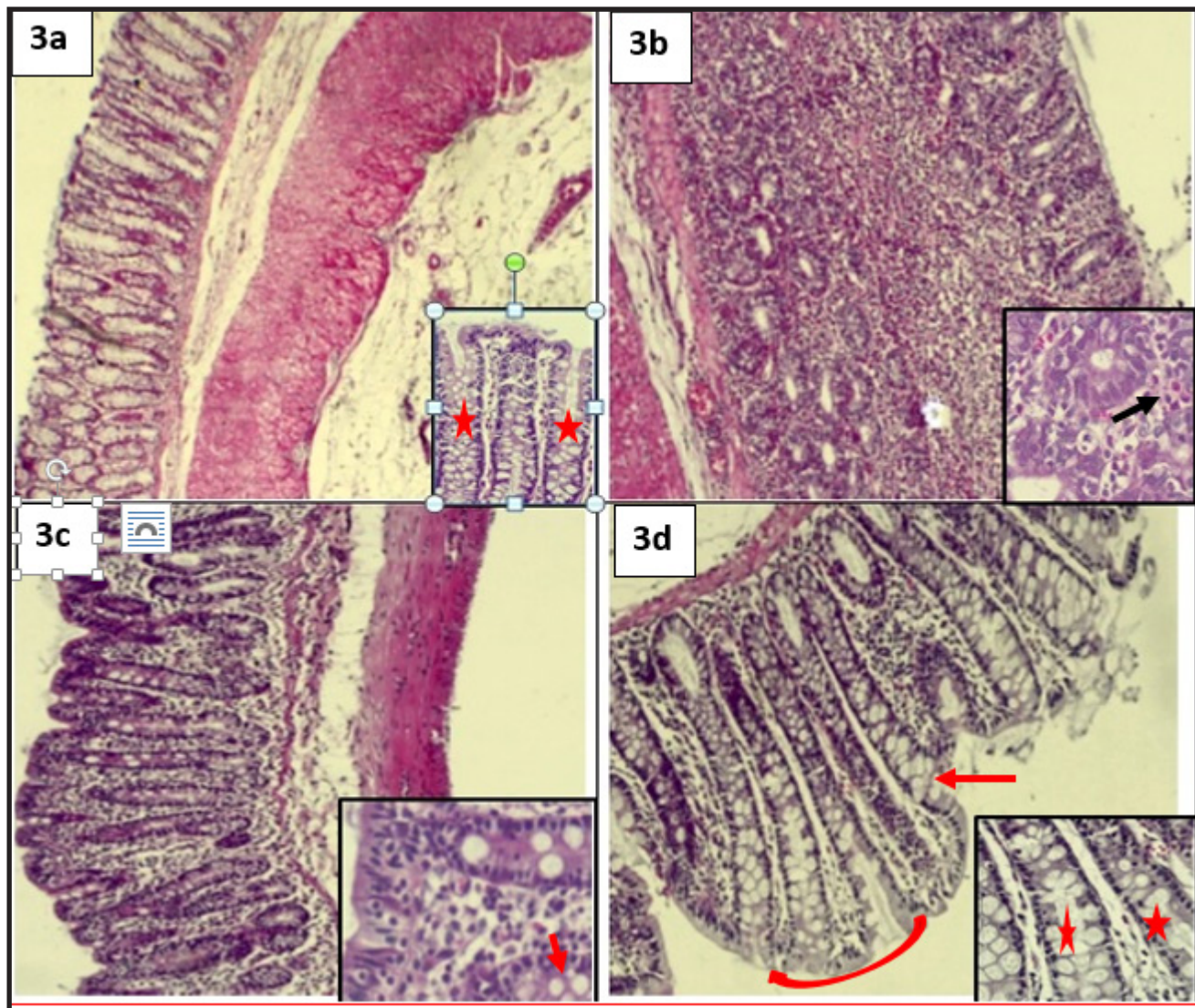


Fig. 3: Photomicrographs of sections in the rat colons of the different groups. Figure 3a, GPI (Control group): closely regular crypt (red *) lined by simple columnar epithelial cells with goblet cells. Figure 3b, GPII (AUC): showing malformed widely spaced crypts with near depletion of goblet cells separated by mixed inflammatory cells rich in eosinophils (black arrow). Figure 3c, GP III (GE treated): showing a normal folded mucosa, near closely regular crypts lined by columnar epithelial cells with a moderate number of goblet cells (red arrow) and fewer inflammatory cells infiltrate. Figure 3d, GPIV (GDNP treated): showing a normal folded mucosa (red curved arrow) closely regular crypts (red *) lined by columnar epithelial cells with a huge number of goblet cells (red arrow) H&E X 200, inset X 400).

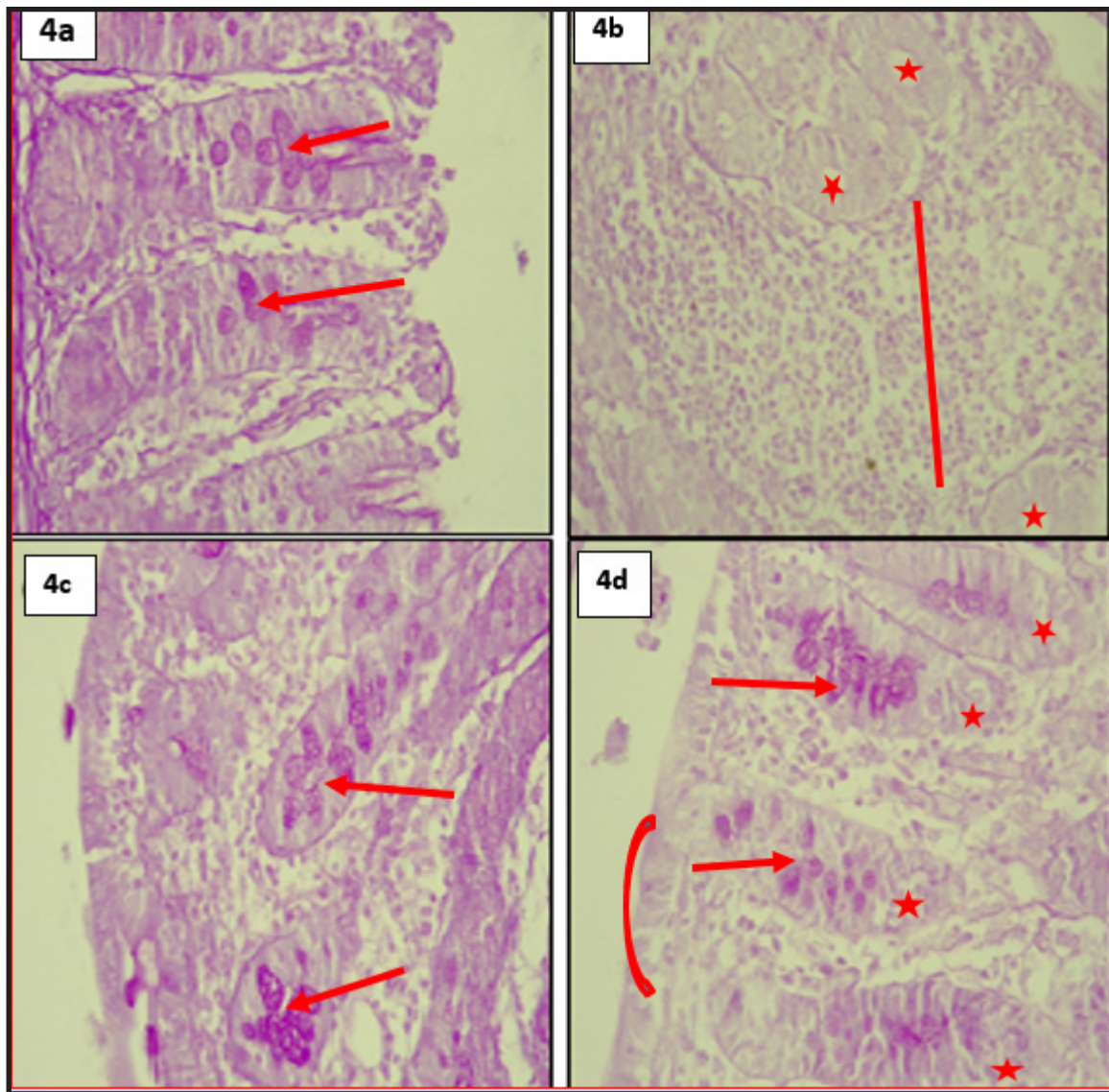


Fig. 4. Photomicrographs of sections in the rat colons of the studied groups. Figure 4a, GP I (Control group): showing closely regular crypt lined by simple columnar epithelial cells with reasonable number of goblet cells (red arrow) (Mean=19/HPF). Figure 4b, GP II (AUC): showing malformed widely spaced crypts (red * and red line) with near depletion of goblet cells (Mean=0.4/HPF). Figure 4c, GP III (GE treated) showing normal folded mucosa, near closely regular crypts lined by columnar epithelial cells with a moderate number of goblet cells (red arrow) (Mean=33/HPF). Figure 4d, GP IV (GDNP treated): showing a folded mucosa (red curved line), closely regular crypts (red*) lined by columnar epithelial cells with a huge number of goblet cells (red arrow) (Mean=73/HPF). PAS X 400

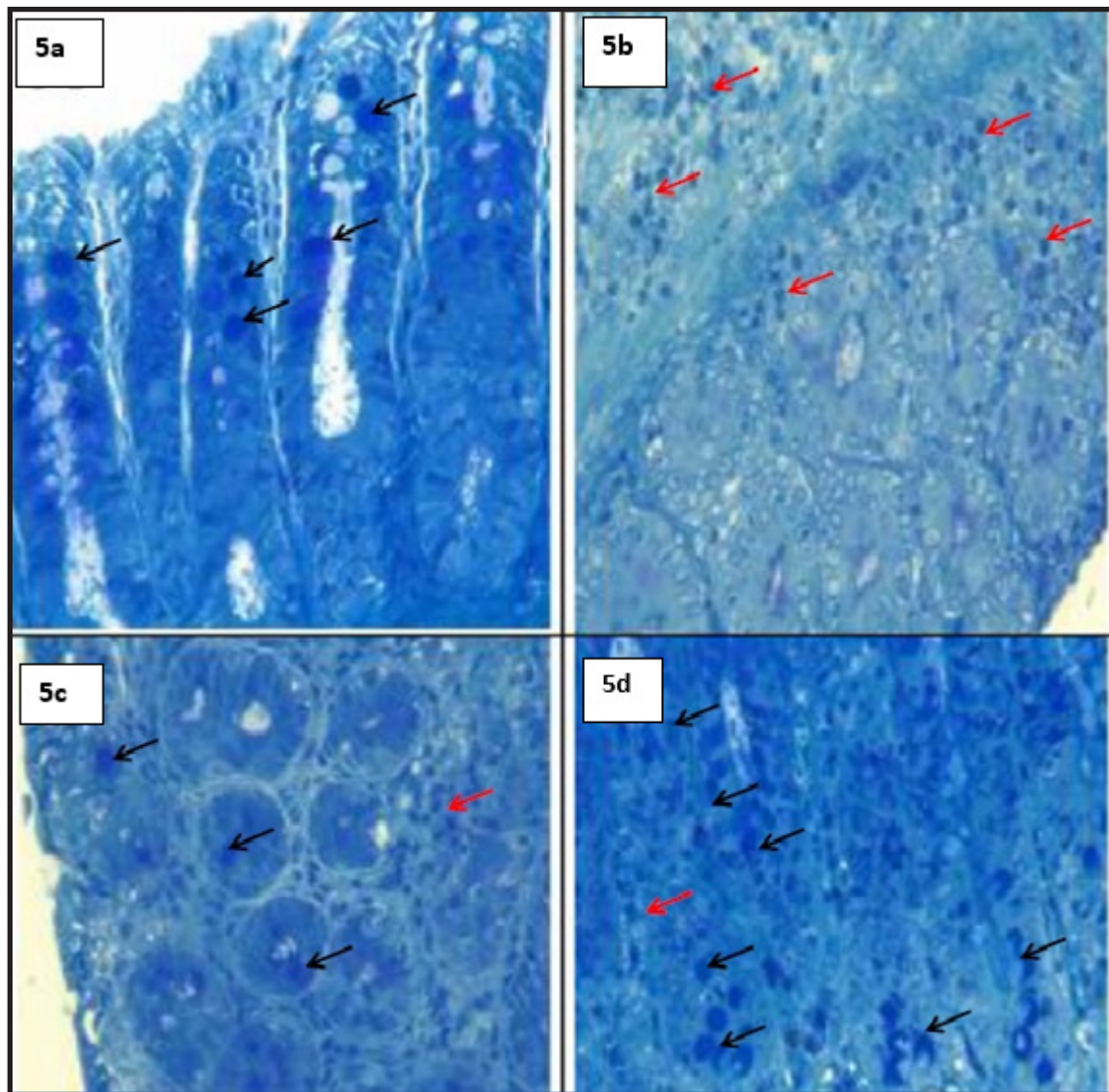


Fig. 5: Photomicrographs of sections in the rat colon of the studied groups. Figure 5a, GP I (Control): showing a closely regular crypt lined by simple columnar epithelial cells with a moderate number of goblet cells (black arrows) (Mean=19/HPF) and no mast cell infiltration. Figure 5b, GP II (AUC): showing an absence of goblet cells and a heavy mast cell infiltration (red arrow) (Mean=21/HPF). Figure 5c, GP III (GE treated): showing a moderate number of goblet cells (black arrows) (Mean=33/HPF) and slight mast cell infiltration (red arrow) (Mean=11/HPF). Figure 5d, GP IV (GDNP treated): showing a huge number of goblet cells cup shaped appearance (black arrows) (Mean=73/HPF) and a very little mast cell infiltration (red arrow) (Mean=7/HPF). Toluidine Blue X 400.

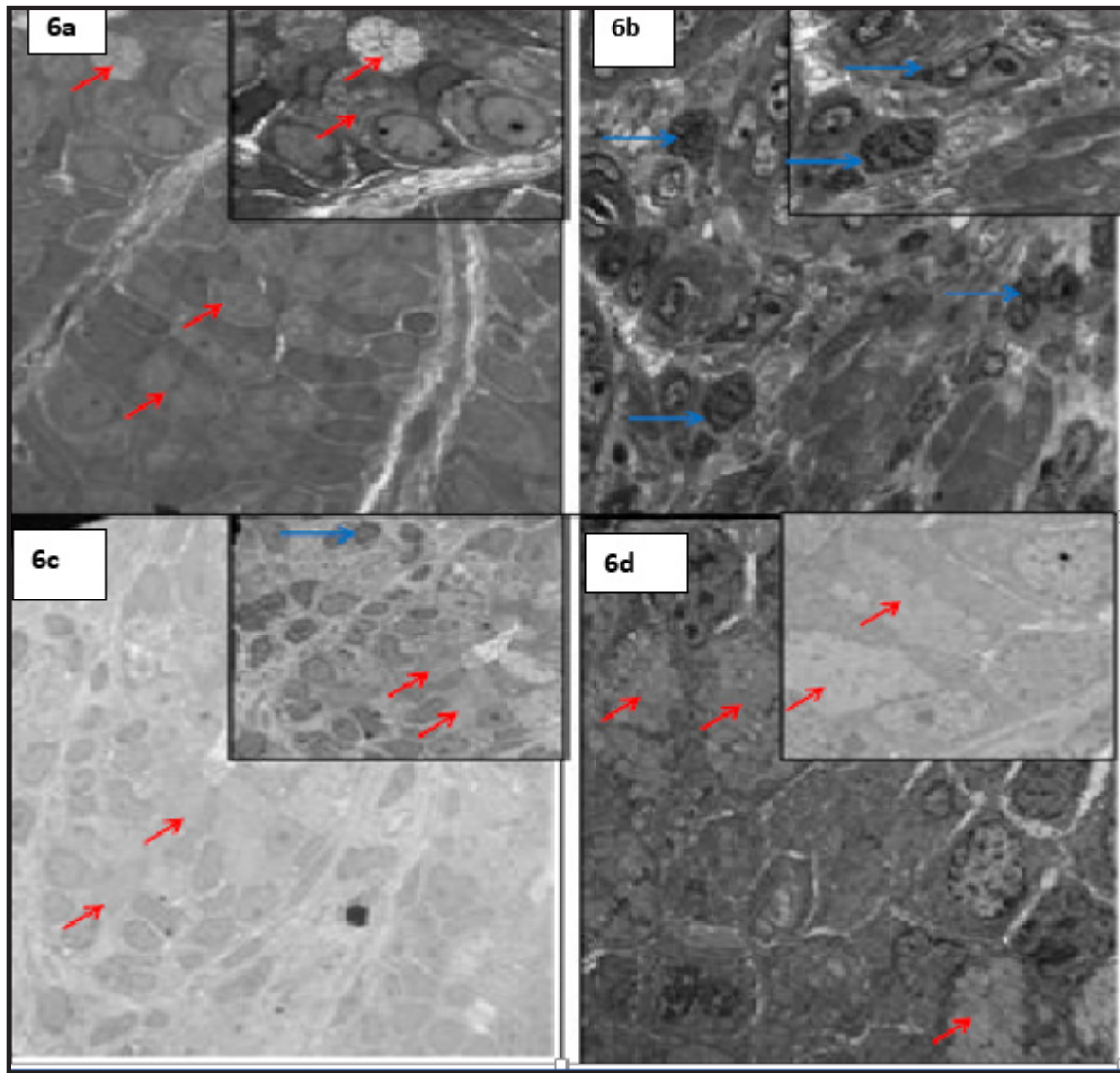


Fig. 6: Photoelectron micrographs of sections in the colon shown by electron microscopy of of the resected colon of the studied groups. GP I (control): shows an intact crypt lined by simple columnar epithelial cells with reasonable number of goblet cells (red arrows). GP II (AUC): shows absent goblet cells and heavy neutrophilic (segmented) nuclei and eosinophilic (bilobed nuclei) infiltration around and invading the crypt epithelial cells (blue arrow). GP III (GE treated) shows a moderate number of goblet cells (red arrows) and a little inflammatory cell infiltration (blue arrow, plasma cell with cartwheel nuclei). GP IV (GDNP treated): shows closely packed crypts lined by columnar epithelial cells with huge number of goblet cells cup shaped appearance (red arrows) and no inflammatory cells infiltration. Direct mag X 2000 (inset X 5000)

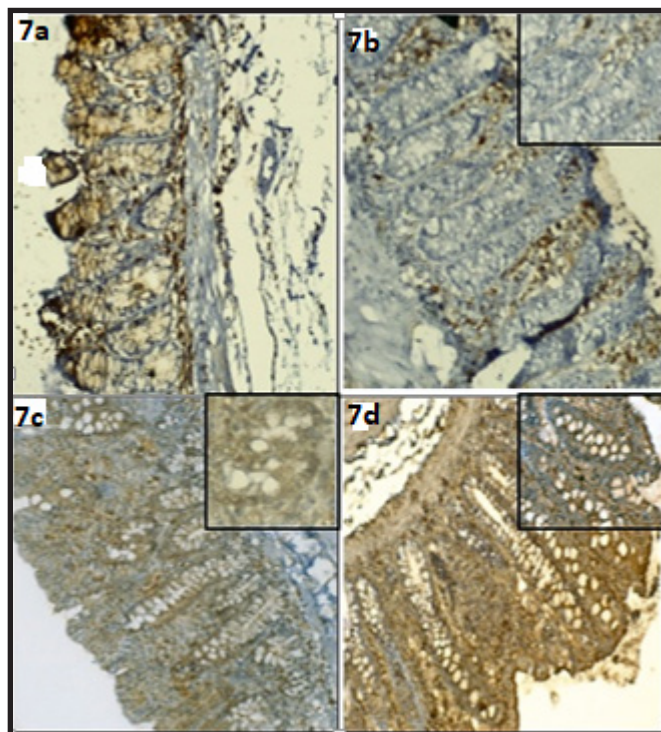


Fig. 7: Photomicrographs of sections of an immunohistochemistry of the rat colon labeled with KI67 antibody of the studied groups. Figure 7a, GPI (control): showing a positive moderate nuclear staining in 20%/HPF. Figure 7b, GPII (AUC): showing a weak positive nuclear staining (5%/HPF) mostly sparing the crypt. Figure 7c: GPIII (GE treated): showing a moderate positive nuclear staining in 50%/HPF. Figure 7d: GP IV (GDNP treated): showing a strong positive nuclear staining in 66%/HPF. X 200, and inset X 400

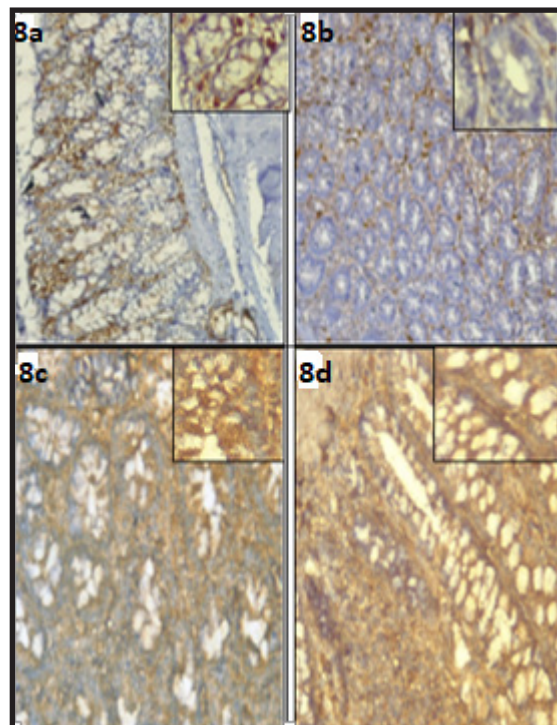


Fig. 8: Photomicrographs of sections of an immunohistochemistry of the rat colon labeled with BCL2 antibody of the studied groups. Figure 8a GPI (Control): showing a moderate positive nuclear and cytoplasmic staining in 25%/HPF. Figure 8b GP II (AUC): showing a weak positive nuclear and cytoplasmic staining (8%/HPF) mostly sparing the crypt. Figure 8c GP III (GE treated): showing a moderate positive nuclear and cytoplasmic staining in 60%/HPF. Figure 8d, GP IV (GDNP treated): showing a strong positive nuclear and cytoplasmic staining in 76%/HPF. X 200, and inset X 400.

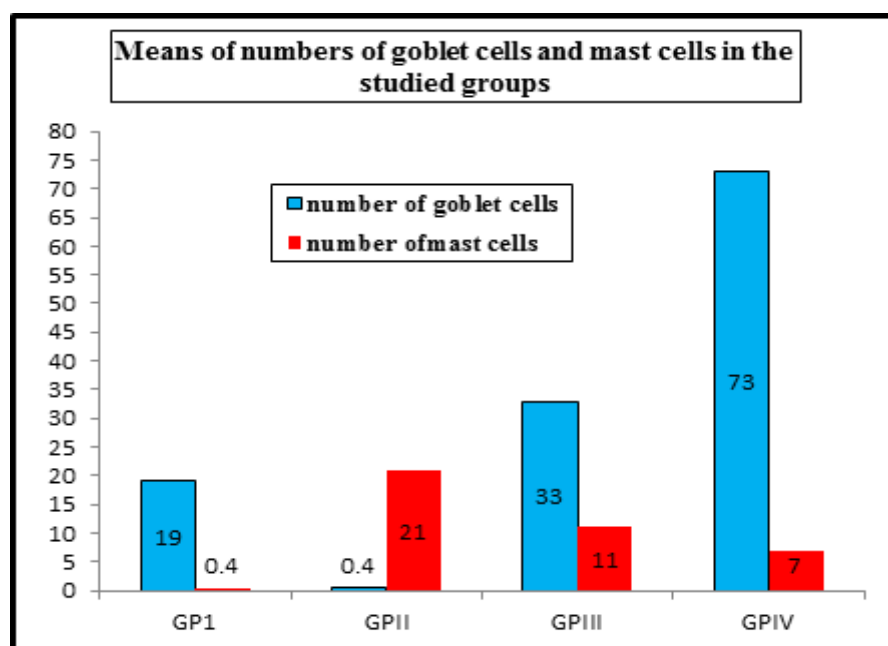


Fig. 9: A histogram showing means of numbers of goblet and mast cells in the studied groups.

Table: Mean value \pm SD of morphological and immunohistochemical parameters of the studied groups and its significance

group	Gross damage score	Histological score	Mean number Goblet cells	Mean number Mast cells	KI-67 +ve ratio	BCL2+ve ratio	<i>P</i> value
GPI (control)	0 \pm 0	0 \pm 0	19.4 \pm 3.7	0.4 \pm 0.5	20 \pm 7	25 \pm 8	0.000
GPII (AUC)	2.6 \pm 1.1	9.2 \pm 3.3	0.4 \pm 0.5	21 \pm 6.2	5 \pm 3.6	8 \pm 4.6	0.000
GP3 (GE treated)	1.4 \pm 1.1	3 \pm 1.6	33 \pm 5.4	11.6 \pm 2.7	50 \pm 15	60 \pm 16	0.000
GPIV (GDNP treated)	0 \pm 0	1 \pm 1	73 \pm 9.7	7 \pm 1.5	66 \pm 8	76 \pm 9	0.000

DISCUSSION

In Egypt, UC poses a big burden on the health sector due to the acute rise of its incidence. In addition, there is a need for a lifelong treatment that is both expensive and with many toxic side-effects. Ginger loaded nanoparticles (GDNP) therapy alleviate colitis signs and accelerate wound repair in DSS-induced colitis rat model. Targeted drug delivery particularly nanoparticle-based drug may provide a better outcome UC treatment. Nanoparticle-based drug delivery systems (DDSs) may protect a loaded drug from environmental degradation and locally increase the concentration of the drug^[4,19].

In this study we induced UC by DSS in addition to ethanol 50% from day 4 to 7 as the clinical course, site of the lesions and morphological features in this model is similar to human UC and to some extent is inexpensive^[24]. Clinically, our model exhibited characteristic manifestations of UC (remittent diarrhea and bloody stool) (GP II, III, and IV). These manifestations were improved within one week of treatment with either ginger alone or GNP (GP III, and GP IV). Thus, ginger extract and GNPs alleviate colitis symptoms in DSS-induced colitis^[19].

Significant variation of scores of gross appearance damage were noticed among GP I and G IV (0 \pm 0) and GPII,

GP3 (2.6 \pm 1.1, 1.4 \pm 1.1 respectively) (Figure 2, Table). This result was in agreement to previous studies^[11-13]. The gross damage was not marked in this study compared to Chen et al, (2007) study, this may be due to lower concentrations of DSS used in our model. DSS is very expensive, and we used it at a lower concentration (2%) and tried to augment the inflammatory effect of DSS (2%) by adding ethanol from day 3. In our study we found that ethanol less than 50% cannot cause any change of the stool in rats. DSS at a lower concentration can activate the immune response through upregulation of cytokine without causing damage to the mucosa. Chen et. al. (2007) reported that a higher concentration of DSS can cause damage through direct cytotoxicity and interference with the normal interaction between intestinal lymphocytes and epithelial cells in addition to change in the intestinal microflora and increase in the number of Gram-negative anaerobes^[24,30]. Intrarectal administration of alcohol helps the process of inflammation and ulceration through upregulation of both interferon gamma (IFN- γ) and interleukin-4 (IL-4) production by the cecal lymph node (nodes) and the splenic cells^[24,31]. Also, ethanol can destroy the colonic epithelium that is responsible for maintenance of mucosal homeostasis and then exposure to fecal antigens^[24,32].

The repair effect of ginger and GDNPs in our study were consistent with the results of previous Zhang *et al* studies^[11,19,22]. The healing effect of ginger and GDNPs can be explained by enhancing the survival and proliferation of the epithelial cells and reducing the pro-inflammatory cytokines (TNF- α , IL-6, and IL-1 β), and increasing the anti-inflammatory cytokines (IL-10 and IL-22) in AUC models, suggesting that GDNPs has the potential to attenuate the damaging factors while promoting the healing effect^[11,19,33].

Our histopathological results show that the treatment with ginger extract and GDNPs reduces inflammatory cell infiltration and increases the number of goblet cells. We found that GDNPs exerts more potent anti-inflammatory effects and attenuate DSS-induced UC than of ginger extract (Figures 3c and 3d). Examination of colonic sections from GP II (AUC model) showed erosion of the mucosa; near absence of goblet cells, and malformed widely spaced crypts (Figure 3b). Mixed inflammatory cells infiltration in the mucosa and in the submucosa was present particularly neutrophils and eosinophils (Figure 3b inset). These findings are consistent with previous studies^[7,10,24]. The sections prepared from the colon of the ginger treated acute UC group (GP III) and the ginger loaded with nanoparticle treated acute UC group (GP IV) showed mostly the same pattern (normal folded mucosa lined by surface columnar epithelial cells). However, the difference was in the distribution of inflammatory cells which is totally absent in GP IV and the number of goblet cells, which is higher in GP IV than GP III. (Figures 3c and, 3d). The cumulative histopathological colitis scores showed significant variation among studied groups with the lowest score was found in GP IV (GDNP) and highest score was in GP II (AUC model) with P =0.000 (Table). These results confirm the advantage of using GDNPs than ginger alone as therapeutic approach for treating UC which were in agreement of other studies using the active component of ginger (6- shogaols) and whole extract of ginger as in our study^[11,19,22].

In this study, treatment with ginger extract (GP III), significantly increased number of goblet cells was observed. This increase was the highest value with GDNPs (GP IV). The numbers of goblet cells in the mucosa of rats with AUC was significantly reduced compared to the control group (Figures 3, 4, 5, 6, 9 and Table). This reduction was confirmed morphometrically and was in agreement with Nowarski *et al.* (2015) study^[34]. These results support the role of ginger in particular GDNPs in repair of AUC which confirm previous studies^[19,22,33]. Goblet cells play an important defensive role in the intestine by their mucin secretion. The colonic mucus plays a main protective role against chemically induced ulceration and assists the repair of the damaged epithelium^[19,22,33].

There was a significant reduction in the inflammatory cells after treatment by ginger and a highest reduction occurred with the use of GDNPs (Figures 3, 4, 7, 5 and 9, Table). There was a heavy infiltration of the mucosa and submucosa with mixed inflammatory cells rich

in eosinophils, neutrophils and mast cells in GP II (AUC) compared to the control group. These results come in accordance with previous studies^[7,8,11,19,22,33]. Inflammatory cells play a critical role in the pathogenesis of UC. The epithelial disruption in AUC is attributed to the inflammatory cytokine (IL1, TNF- α) released from both neutrophils and macrophages. Also Mast cells release histamine and eosinophil chemotactic factor that explain the heavy eosinophilic infiltration in UC^[2,7,8,35]. The reduction of these cells observed in our study support the role of ginger in repair of UC and more pronounced effect with the use of GDNPs.

We finally wanted to address the impact of these cellular changes on the pathogenesis of AUC and repair process observed with ginger treatment. We found that in groups treated with either ginger extract (GP III), and or GDNP (GP IV) epithelial proliferative activity detected by antiKI-67 antibody increased while apoptosis detected by anti BCL2 antibody was decreased. The highest proliferative activity and lowest apoptotic activity was observed in GP IV(GDNPs) (Table, and Figures 7,8,10). This pattern of proliferation and apoptosis confirms that GDNPs treatment exerts a dramatic effect in repair of AUC. These results confirm previous reports on ginger and GDNPs in other models^[11,19,22,33].

Our results also suggest that disruption in the balance between epithelial cell apoptosis and proliferation has a role in the pathogenesis and repair of AUC. The observed high apoptotic and low proliferative activity in GP II (AUC) further supports this idea. Our result is consistent with Araki *et al.*(2010) study in which DSS induced apoptosis of epithelial cells resulted in erosion /ulceration of the epithelium^[36].

CONCLUSION AND RECOMMENDATION

GDNPs clinically, histologically, improved signs of AUC in DSS/Ethanol rat model. It also reduced the apoptosis and enhanced the repair process. Further pharmacological and clinical studies are recommended to evaluate its protective effect and its role in acute and chronic ulcerative colitis in humans and assess its therapeutic efficacy.

CONFLICT OF INTERESTS

There are no conflicts of interest.

REFERENCES

1. Lee Clapper M, Cooper HS, Chang W-CL. Dextran sulfate sodium-induced colitis-associated neoplasia: a promising model for the development of chemopreventive interventions 1. *Acta Pharmacol Sin.* 2007;28:1450-9.
2. Vinay Kumar Stanley L. Robbins ; with illustrations by James A. Perkins. (2003). RSC. Robbins basic pathology. 2017.

3. Molodecky NA, Panaccione R, Ghosh S, Barkema HW, Kaplan GG. Challenges associated with identifying the environmental determinants of the inflammatory bowel diseases. *Inflammatory Bowel Diseases*. 2011;17:1792-9.
4. Esmat S, El Nady M, Elfekki M, Elsharif Y, Naga M. Epidemiological and clinical characteristics of inflammatory bowel diseases in Cairo, Egypt. *World Journal of Gastroenterology*. 2014;20:814-21.
5. Randhawa PK, Singh K, Singh N, Jaggi AS. A review on chemical-induced inflammatory bowel disease models in rodents. *The Korean journal of physiology & pharmacology : official journal of the Korean Physiological Society and the Korean Society of Pharmacology: Korean Physiological Society and Korean Society of Pharmacology*; 2014. p. 279-88.
6. Lombardi VRM, Etcheverría I, Carrera I, Cacabelos R, Chacón AR. Prevention of chronic experimental colitis induced by dextran sulphate sodium (DSS) in mice treated with FR91. *Journal of biomedicine & biotechnology*. 2012;2012:826178.
7. Ismail DI, and A. G. Aboulkhair. Royal jelly protects against experimentally-induced ulcerative colitis in adult male albino rats : A histological study. *The egyptian journal of histology*. 2018;41(2):192-203.
8. Al-Rejaie SS, Abuhashish HM, Al-Enazi MM, Al-Assaf AH, Parmar MY, Ahmed MM. Protective effect of naringenin on acetic acid-induced ulcerative colitis in rats. *World Journal of Gastroenterology* 2013;19:5633-44.
9. Tahan G, Aytac E, Aytekin H, Gunduz F, Dogusoy G, Aydin S, *et al.* Vitamin e has a dual effect of anti-inflammatory and antioxidant activities in acetic acid-induced ulcerative colitis in rats. *Canadian Journal of Surgery*. 2011;54:333-8.
10. D'Errico A MD. Diagnosis of Ulcerative Colitis: Morphology and Histopathological Characteristics. 2019:61-92.
11. Zhang M, Viennois E, Prasad M, Zhang Y, Wang L, Zhang Z, *et al.* Edible ginger-derived nanoparticles: A novel therapeutic approach for the prevention and treatment of inflammatory bowel disease and colitis-associated cancer. *Biomaterials*. 2016;101:321-40.
12. Fukata M, Shang L, Santaolalla R, Sotolongo J, Pastorini C, España C, *et al.* Constitutive activation of epithelial TLR4 augments inflammatory responses to mucosal injury and drives colitis-associated tumorigenesis. *Inflammatory Bowel Diseases*. 2011;17:1464-73.
13. Date AA, Hanes J, Ensign LM. Nanoparticles for oral delivery: Design, evaluation and state-of-the-art. *J Control Release*. 2016;240:504-26.
14. Chan EWC, Lim YY, Wong LF, Lianto FS, Wong SK, Lim KK, *et al.* Antioxidant and tyrosinase inhibition properties of leaves and rhizomes of ginger species. *Food Chemistry*. 2008;109:477-83.
15. Al-Saffar FJ GS, Fakurazi S, Yaakub H and Lip M (2010): Chondroprotective effect of Zerumbone on Monosodium Iodoacetate induced osteoarthritis in rats. *Journal of Applied Sciences*, 10 (4): 248 - 260. . Chondroprotective effect of Zerumbone on Monosodium Iodoacetate induced osteoarthritis in rats. . *Journal of Applied Sciences*., 2010;10(4):248-60.
16. Zivanovic S, Rackov LP, Zivanovic A, Jevtic M, Nikolic S, Kocic S. Cartilage oligomeric matrix protein - inflammation biomarker in knee osteoarthritis. *Bosn J Basic Med Sci*. 2011;11(1):27-32.
17. Ojewole JA. Analgesic, antiinflammatory and hypoglycaemic effects of ethanol extract of *Zingiber officinale* (Roscoe) rhizomes (*Zingiberaceae*) in mice and rats. *Phytother Res*. 2006;20(9):764-72.
18. al-Yahya MA, Rafatullah S, Mossa JS, Ageel AM, Parmar NS, Tariq M. Gastroprotective activity of ginger *zingiber officinale rosc.*, in albino rats. *Am J Chin Med*. 1989;17(1-2):51-6.
19. Zhang M, Xu C, Liu D, Han MK, Wang L, Merlin D. Oral Delivery of Nanoparticles Loaded With Ginger Active Compound, 6-Shogaol, Attenuates Ulcerative Colitis and Promotes Wound Healing in a Murine Model of Ulcerative Colitis. *J Crohns Colitis*. 2018;12(2):217-29.
20. Anosike CA OO, Ezeanyika LUS, Nwuba MM. . Anti-inflammatory and anti-ulcerogenic activity of the ethanol extract of ginger (*Zingiber Officinale*). . *Afr J Biochem Res* 2009;3(12):379-84.
21. Aboul Fotouh GI, Abdel-Dayem MM, Ismail DI, Mohamed HH. Histological Study on the Protective Effect of Endogenous Stem Cell Mobilization in Busulfan-Induced Testicular Injury in Albino Rats. *J Microsc Ultrastruct*. 2018;6(4):197-204.
22. Zhang M, Merlin D. Nanoparticle-Based Oral Drug Delivery Systems Targeting the Colon for Treatment of Ulcerative Colitis. *Inflamm Bowel Dis*. 2018;24(7):1401-15.
23. Huang Z, Gan J, Jia L, Guo G, Wang C, Zang Y, *et al.* An orally administrated nucleotide-delivery vehicle targeting colonic macrophages for the treatment of inflammatory bowel disease. *Biomaterials*. 2015;48:26-36.
24. Chen Y, Si JM, Liu WL, Cai JT, Du Q, Wang LJ, *et al.* Induction of experimental acute ulcerative colitis in rats by administration of dextran sulfate sodium at low concentration followed by intracolonic administration of 30% ethanol. *J Zhejiang Univ Sci B*. 2007;8(9):632-7.

25. Eid MM, El-Hallouty SM, El-Manawaty M, Abdelzaher FH. Physicochemical characterization and biocompatibility of spion@plasmonic @chitosan core-shell nanocomposite biosynthesized from fungus species. *Journal of Nanomaterials*. 2019;2019.
26. M.E. Osman O.H. Khattab SME-HD, M M Eid. Biosynthesis of silver nano-particles by local fungal isolates from egyptian soil. *Quantum Matter*. 2016;5:305-11.
27. Eid MM, El-Hallouty SM, El-Manawaty M, Abdelzaher FH, Al-Hada M, Ismail AM. Preparation conditions effect on the physico-chemical properties of magnetic-plasmonic core-shell nanoparticles functionalized with chitosan: Green route. *Nano-Structures and Nano-Objects*. 2018;16:215-23.
28. M.E. Osman O.H. Khattab SMA-EA, S.M. El-Hallouty DAM., M M Eid. Optimization and spectroscopic characterization of the biosynthe- sized silver/chitosan nanocomposite from aspergillus deflectus and penicillium pinophilum. *J Chem Biol Phys Sci*. 2015;5:2643.
29. Zhao X ZH, Chen J, and Ao Q. FTIR , XRD and SEM Analysis of Ginger Powders with Different Size. *J Food Process Preserv*.39(6):2017-26.
30. Vicario M, Crespí M, Franch À, Amat C, Pelegrí C, Moretó M. Induction of colitis in young rats by dextran sulfate sodium. *Digestive Diseases and Sciences*. 2005;50:143-50.
31. Andrade MC, Vaz NM, Faria AMC. Ethanol-induced colitis prevents oral tolerance induction in mice. *Brazilian Journal of Medical and Biological Research*. 2003;36:1227-32.
32. New concepts in the pathophysiology of inflammatory bowel disease, (2005).
33. Kim MS, Kim JY. Ginger attenuates inflammation in a mouse model of dextran sulfate sodium-induced colitis. *Food Sci Biotechnol*. 2018;27(5):1493-501.
34. Nowarski R, Jackson R, Gagliani N, De Zoete MR, Palm NW, Bailis W, *et al*. Epithelial IL-18 Equilibrium Controls Barrier Function in Colitis. *Cell*. 2015;163:1444-56.
35. Lorentz A, Sellge G, Bischoff SC. Isolation and characterization of human intestinal mast cells. *Methods Mol Biol*. 2015;1220:163-77.
36. Araki Y, Mukaisyo K, Sugihara H, Fujiyama Y, Hattori T. Increased apoptosis and decreased proliferation of colonic epithelium in dextran sulfate sodium-induced colitis in mice. *Oncol Rep*. 2010;24(4):869-74.

الملخص العربي

التأثير النسيجي المرضي للجسيمات النانوية المحملة بالزنجبيل مقابل مستخلص الزنجبيل كعلاج جديد لالتهاب القولون التقرحي الحاد التجريبي

منال حمدي البدوي^١، نرمين عصمت والي^٢، مي محمد عيد^٣، ناهد أحمد سليمان^٤

^١قسم التشريخ الأدمى وعلم الأجنه، ^٢قسم الفسيولوجى، ^٣قسم الباثولوجى، كلية الطب - جامعه حلوان

^٤قسم التحليل الطيفى - فيزياء - المركز القومى للبحوث

الخلفية: التهاب القولون التقرحي (UC) هو مرض التهاب الأمعاء المزمن الذي ينتشر في مصر. العلاج الحالي لالتهاب التقرحي باهظ الثمن وله آثار جانبية خطيرة.

الهدف من العمل: لتقييم تأثير الجسيمات النانوية المحملة بالزنجبيل (GDNP) مقارنة بمستخلص الزنجبيل (GE) كعلاج بديل لالتهاب التقرحي الحاد والقولون المتمثل في النموذج الناشئ عن استخدام DSS / الإيثانول بالفئران. **المواد والطرق:** تم استخدام عشرين فأراً. تم تحفيز AUC عن طريق إعطاء 2 ٪ ديكستران كبريتات الصوديوم الاصطناعية (DSS). تم تقسيم الفئران إلى 4 مجموعات: مجموعة التحكم (GP II) AUC ، (GP I) ، تلقت 2.5 جم 2.5 ، (GP III) GE من الجسيمات النانوية الفائقة (GP VI) (GDNP). تم تقييم نسيج القولون والمستقيم نسيجياً باستخدام H&E و PAS و Toluidine blue والمجهر الإلكتروني (EM). تم تقييم معدل التكاثر والموت المبرمج بواسطة الاجسام المضاد ه لـ KI-67 المضاد لـ BCL2.

النتائج: أظهر GP III و GP IV تحسناً مع GDNP و GE مقارنة بالتحكم. كانت درجات الضرر الإجمالي كما يلي: GP I 0 ± 0 ، GPII 2.6 ± 1.1 ، GPIII 1.4 ± 1.1 ، و GPIV 0 ± 0 مع تباين كبير (P = 0.000). كانت الدرجة التراكمية المرضية النسيجية لـ GP I و GP II و GP III و GP IV هي 0 ± 0 و 3.3 ± 9.2 و 1.6 ± 3 و 1 ± 1 على التوالي (P = 0.000). أظهر GPIV و GPIII تصبغ إيجابياً قوياً لـ KI-67 (متوسط HPF / 50 ± 15). (متوسط HPF / 9 ± 76 و 16 ± 60 = المتوسط) BCL2 و GPIV = 66 ± 8 / HPF مع تباين كبير (P = 0.000). **الخلاصة:** GDNP لديه إمكانات أكبر في علاج التهاب التقرحي الحاد مقارنة بـ مستخلص الزنجبيل. أدى العلاج باستخدام مستخلص الزنجبيل المحمل بالنانو إلى تحسين العلامات وتقليل موت الخلايا المبرمج وتحسين التهاب التقرحي الحاد بالقولون بشكل أكبر من مستخلص الزنجبيل.